Atmospheric carbon dioxide levels for the last 500 million years

Daniel H. Rothman[†]

Department of Earth, Atmospheric, and Planetary Sciences, Massachusetts Institute of Technology, Cambridge, MA 02139

Communicated by Paul F. Hoffman, Harvard University, Cambridge, MA, January 30, 2002 (received for review October 9, 2001)

The last 500 million years of the strontium-isotope record are shown to correlate significantly with the concurrent record of isotopic fractionation between inorganic and organic carbon after the effects of recycled sediment are removed from the strontium signal. The correlation is shown to result from the common dependence of both signals on weathering and magmatic processes. Because the long-term evolution of carbon dioxide levels depends similarly on weathering and magmatism, the relative fluctuations of CO_2 levels are inferred from the shared fluctuations of the isotopic records. The resulting CO_2 signal exhibits no systematic correspondence with the geologic record of climatic variations at tectonic time scales.

The long-term carbon cycle is controlled by chemical weathering, volcanic and metamorphic degassing, and the burial of organic carbon (1, 2). Ancient atmospheric carbon dioxide levels are reflected in the isotopic content of organic carbon (3) and, less directly, strontium (4) in marine sedimentary rocks; the former because photosynthetic carbon isotope fractionation is sensitive to CO_2 levels, and the latter because weathering and degassing are associated with extreme values of the abundance ratio $^{87}Sr/^{86}Sr$. However, attempts to use these geochemical signals to estimate past CO_2 levels (5–8) are hindered by the signals' additional relationships to various tectonic (9, 10) and biological (11) effects. Moreover, the strontium signal has proven especially difficult to parse (12–15).

Here, I attempt to resolve these ambiguities in the isotopic signals of carbon and strontium. First, it is shown that the last 500 million years of the strontium signal, after transformation to remove the effects of recycled sediment (16, 17), correlate significantly with the concurrent record of isotopic fractionation between inorganic and organic carbon (3). This empirical result is supplemented by the theoretical deduction that the two records are linked by their common dependence on rates of continental weathering and magmatic activity. The assumption that CO_2 levels fall with the former and rise with the latter then indicates that an appropriate average of the two records should reflect the long-term fluctuations of the partial pressure of atmospheric CO_2. The CO_2 signal derived from this analysis represents fluctuations at time scales greater than about 10 million years (My). Comparison with the geologic record of climatic variations (18) reveals no obvious correspondence.

Strontium and Carbon Isotopic Signals

Fig. 1 shows the strontium and carbon isotopic signals for the last 500 My. The data for the strontium isotope ratios $^{87}Sr/^{86}Sr$ were compiled by Veizer *et al.* (4) and Walter *et al.* (19); the former source accounts for all $^{87}Sr/^{86}Sr$ data younger than 520 My, whereas the latter was used for data extending back to 608 My (not shown). Both sets of $^{87}Sr/^{86}Sr$ data were first averaged in nonoverlapping time windows of 10 My. The resulting unevenly spaced record was then transformed (20) to an evenly spaced record with time increments of approximately 10 My and no contributions to the power spectral density at periods less than 21 My.

The second record in Fig. 1, compiled by Hayes *et al.* (3) derives from the isotopic composition of marine organic carbon and carbonate carbon. From isotopic abundance ratios $R_x = (^{13}C/^{12}C)_x$ for carbon in sample x, the isotopic fractionation between sample x and a standard (STD) sample, $\delta_x = 1{,}000[(R_x - R_{STD})/R_{STD}]$, is obtained for carbonate (δ_a) and organic (δ_o) carbon. The isotopic fractionation ε_{toc} between total organic carbon and sedimentary carbonates is then given approximately by $\varepsilon_{toc} = \delta_a - \delta_o$, which is the second signal plotted in Fig. 1.

Fig. 1 shows a surprising similarity between the two records for fluctuations with periods less than about 100 My. However, the correlation between the two time series is not statistically significant[‡] [Spearman rank correlation coefficient (21) $R_s = -0.40$, $P = 0.17$, $N = 46$], because the longer-period fluctuations are not in phase. It is therefore interesting to ask why the two records appear similar at shorter time scales and dissimilar at longer time scales.

Recent work has shown that the measurements of ε_{toc} approximately fit the empirical relation (3, 22)

$$\varepsilon_{toc} = \varepsilon_0 - \Gamma/\Phi. \quad [1]$$

The parameter ε_0 represents the isotopic effects of photosynthesis and secondary biological processes along with the isotopic depletion of dissolved CO_2 in surface waters relative to sedimentary carbonate. Because ε_0 is approximately constant throughout the period plotted in Fig. 1, the main source of ε_{toc}'s fluctuations is contained in isotopic effects due to changing algal physiology—the permeability, surface-to-volume ratio, and growth rate of algal cells—represented by Γ, and the concentration Φ of dissolved carbon dioxide in surface waters (3, 8).

Although the mechanisms responsible for the fluctuations of $s = {}^{87}Sr/^{86}Sr$ are subject to much debate (4, 9, 10, 12–15), some aspects of the signal's evolution are nevertheless clear. Because ^{87}Rb decays to ^{87}Sr with a half-life of ~48 billion years, the supply of ^{87}Sr may be taken to be approximately constant over the last 500 My. However, it is not uniformly distributed: the fluvial input to the oceans is derived in part from rocks—both silicates and metamorphosed carbonates (12–15)—that are relatively enriched in radiogenic Sr ($s \simeq 0.712$ or greater) compared to the nonradiogenic Sr of mantle origin supplied at hydrothermal vents ($s \simeq 0.7035$) (23). The value of $s(t)$ at some particular time t represents, to first approximation, the relative fluxes of these two extreme values.

Abbreviation: My, million years.

[†]E-mail: dan@segovia.mit.edu.

[‡]Correlations between $\varepsilon_{toc}(t)$ and $s(t)$ or $g(t)$ are computed from the N equal-time pairs obtained after linearly interpolating the Sr signal so that it is sampled at the same times as ε_{toc}. The statistical significance P is one-sided and was estimated by using the Monte Carlo technique described in ref. 8.

The publication costs of this article were defrayed in part by page charge payment. This article must therefore be hereby marked "*advertisement*" in accordance with 18 U.S.C. §1734 solely to indicate this fact.

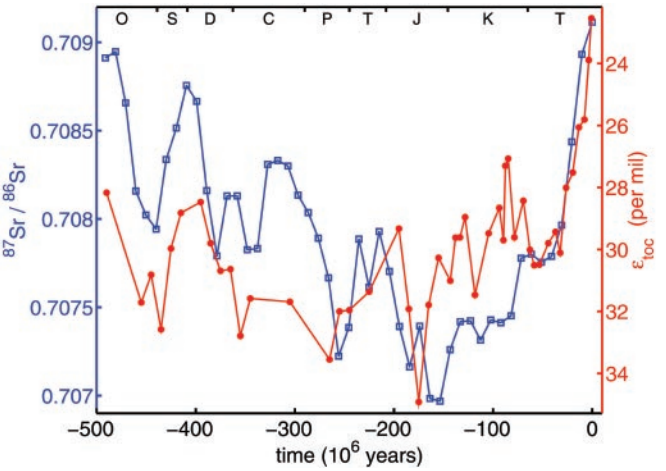

Fig. 1. Data for ε_{toc} (red filled circles) (3) and $^{87}Sr/^{86}Sr$ (blue open squares) (4). The time scale for ε_{toc} has been revised from the original to match the scheme (32) used for the strontium data. The capital letters correspond to the following geologic periods: Ordovician, Silurian, Devonian, Carboniferous, Permian, Triassic, Jurassic, Cretaceous, and Tertiary.

However, this first approximation ignores the recycling of rocks in the sedimentary cycle (16). As pointed out by Brass (17), about 75% of the strontium input to the oceans should come from the weathering of exposed carbonates of marine origin. Because these carbonates retain a memory of s at the time of deposition, their contribution to sedimentary Sr significantly damps the signal coming from hydrothermal vents (low s) and rocks containing radiogenic Sr (high s) (9).

Denoting the fluvial flux of radiogenic Sr by r, the input from hydrothermal vents by v_h, and the memory effect by m, a simple expression for the strontium isotope ratio s is

$$s = \mu m + (1 - \mu)g(r, v_h), \qquad [2]$$

where $0 \leq \mu \leq 1$ is the fraction of sedimentary Sr deriving from the memory flux, and g is a function that depends on both r and v_h. The memory term can be approximated by assuming that sedimentary strontium is weathered at a rate proportional to its mass (16). Then $m(t)$ is simply a weighted (exponentially decaying) average of $s(\tau)$, $\tau < t$ (17), which we express by the convolution

$$m(t) = \int_{-\infty}^{t} \lambda e^{-\lambda(t-\tau)} s(\tau) \mathrm{d}\tau. \qquad [3]$$

The parameter λ is related to the half-life $t_{1/2}$ of sedimentary Sr; i.e., $\lambda = -(\ln 2)/t_{1/2}$. Brass estimates 57 My $< t_{1/2} <$ 102 My (17). Therefore, the memory effect should strongly influence the fluctuations of s at long time scales (greater than about 100 My), whereas the short time scale fluctuations should be relatively unaffected.

The short-time correlations may be explained in part by noting the common dependence of ε_{toc} and g on the global weathering rate w (i.e., the flux of all weathered products from the continents to the oceans) and the rate of magmatic activity v associated not only with the hydrothermal flux v_h but also with volcanic degassing. Assuming that $r = r(w)$ and $v_h = v_h(v)$, g's dependence on w and v may be written[§]

$$g = g(r(w), v_h(v)). \qquad [4]$$

With respect to ε_{toc}, the physiological term Γ may likewise depend on w because of changing nutrient concentrations in the oceans. Γ could also depend on CO_2 levels, which in turn depend on degassing, weathering rates—because of the net uptake rate $u = u(w)$ of atmospheric CO_2 associated with silicate weathering (1, 2, 24)—and other processes, such as organic carbon burial, which we collectively designate by b. Aggregating these dependencies then yields

$$\varepsilon_{toc} = \varepsilon_0 - \frac{\Gamma(w, \Phi(u(w), v, b))}{\Phi(u(w), v, b)}. \qquad [5]$$

Comparison of Eqs. **4** and **5** directly reveals the joint dependence of g and ε_{toc} on v and w.

Removal of the Effects of Sedimentary Recycling

Because the strontium signal s contains a memory effect, whereas ε_{toc} does not, removal of the memory effect should reveal correlations between s and ε_{toc} at both short and long time scales, thereby confirming the joint dependence on v and w. To test this hypothesis, I first assume it is true and use it to estimate g. For a given λ and μ, m is calculated by discretizing Eq. **3** for $\tau > -608$ My. Eq. **2** is then solved for g:

$$g_{\lambda\mu} = \frac{s - \mu m_\lambda}{1 - \mu}. \qquad [6]$$

Here the subscripts make explicit the dependencies on λ and μ.

Let $R_{\lambda\mu}(\varepsilon_{toc}, g_{\lambda\mu})$ be the Pearson product-moment correlation coefficient (21) that quantifies the similarity of ε_{toc} and $g_{\lambda\mu}$. From the foregoing argument, the best estimate of λ and μ should be that which minimizes $R_{\lambda\mu}$ (because the expected correlation is negative). Fig. 2 shows contours of R as a function of μ and $t_{1/2} = -(\ln 2)/\lambda$. The minimum $R_{\lambda\mu} = -0.81$ occurs at $t_{1/2} = 54$ My and $\mu = 0.99$. However, the corresponding estimate of $g_{\lambda\mu}$ includes values below the hydrothermal minimum of 0.7035. Such nonphysical ratios probably derive from the amplification of any measurement noise resulting from division by the small quantity $1 - \mu$ in Eq. **6**. Indeed, the dark gray region in Fig. 2 indicates that all such results occur only for μ close to unity. I therefore define the best estimates λ^*, μ^* of λ, μ by minimizing $R_{\lambda\mu}$ subject to the constraint that $g_{\lambda\mu} > 0.7035$. One then finds $t^*_{1/2} = -\ln 2/\lambda^* = 41$ My and $\mu^* = 0.83$, corresponding to $R_{\lambda^*\mu^*} = -0.80$ (within 1% of the unconstrained minimum). These results are in reasonable accord with Brass's estimate of the half-life of sedimentary Sr (57 − 102 My) (17) and his conclusion that "strontium leached from limestones is about 75% of the total input" (17).

Fig. 3 shows $g_{\lambda^*\mu^*}$ compared to ε_{toc}. Compared with Fig. 1, one sees that both the long and short period fluctuations are now not only approximately equally correlated, but the correlation is also significant ($R_s = -0.74$, $P < 10^{-3}$, $N = 46$). The hypothesis that recycled sediment partially obscured an inherent correlation because of a shared dependence on weathering and volcanic processes is therefore confirmed.

Relationship to CO_2 Levels

To understand further the correlation, I make the following assumptions concerning the functional dependencies contained in Eqs. **4** and **5**:

$$\mathrm{d}r/\mathrm{d}w > 0, \quad \mathrm{d}u/\mathrm{d}w > 0, \quad \text{and} \quad \mathrm{d}v_h/\mathrm{d}v > 0. \qquad [7]$$

The first two state that the flux of radiogenic Sr to the oceans and the uptake of atmospheric CO_2 because of silicate weathering increase as the global weathering rate (of all minerals in all

[§]Although w and v could conceivably depend on one another, here such dependencies are assumed to be insignificant compared to any independent variations.

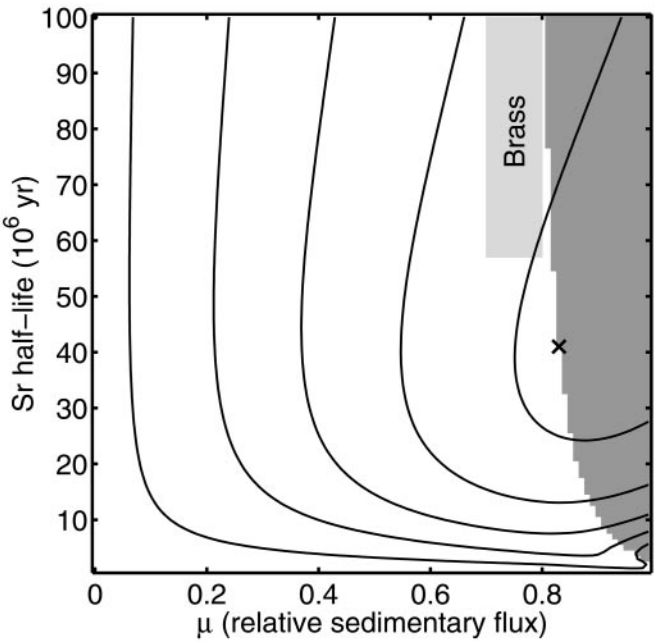

Fig. 2. Contours of $R_{\lambda\mu}$ as a function of μ, the fraction of sedimentary Sr deriving from the memory flux, and $t_{1/2} = -(\ln 2)/\lambda$, the half-life of sedimentary Sr. R was calculated for $\mu = 0, 0.01, \ldots, 0.99$ and $t_{1/2} = 1, 2, \ldots, 99$ My. For large half-life, the contours decrease from left to right as follow: -0.60, -0.65, -0.70, -0.75, -0.79. The symbol $\times$ marks the minimum, $R_{\lambda^*\mu^*} = -0.80$, obtained under the constraint that $g(t) > 0.7035$. The area shaded dark gray on the right does not satisfy the constraint. The rectangular area labeled "Brass" corresponds to previous estimates obtained by geochemical arguments (17); its horizontal extent has not been explicitly computed.

terranes) increases. The third formalizes the natural assumption that the hydrothermal flux of Sr varies with the same sign as all magmatic processes.

Because the Sr isotope ratios increase with increasing r (i.e., $\partial g/\partial r > 0$) and decrease with increasing v_h (i.e., $\partial g/\partial v_h < 0$), one has

$$\frac{\partial g}{\partial v} = \frac{\partial g}{\partial v_h}\frac{\mathrm{d}v_h}{\mathrm{d}v} < 0 \quad \text{and} \quad \frac{\partial g}{\partial w} = \frac{\partial g}{\partial r}\frac{\mathrm{d}r}{\mathrm{d}w} > 0. \qquad [8]$$

Because g and $\varepsilon_{\mathrm{toc}}$ are negatively correlated, one expects that $\varepsilon_{\mathrm{toc}}$ depends on v and w in the opposite sense:

$$\partial\varepsilon_{\mathrm{toc}}/\partial v > 0 \quad \text{and} \quad \partial\varepsilon_{\mathrm{toc}}/\partial w < 0. \qquad [9]$$

The inequalities **8** and **9** have been obtained without making any explicit assumption concerning any dependence of r on u nor Γ on v and w. Because they show that v and w each influence g and $\varepsilon_{\mathrm{toc}}$ with opposite signs, the relative fluctuations of any other quantity that also depends on v and w with opposite signs may be inferred from the shared fluctuations of g and $\varepsilon_{\mathrm{toc}}$.[¶] Specifically, the concentration Φ of oceanic CO_2 responds positively to v while its response to weathering is negative:

$$\frac{\partial\Phi}{\partial v} > 0 \quad \text{and} \quad \frac{\partial\Phi}{\partial w} = \frac{\partial\Phi}{\partial u}\frac{\mathrm{d}u}{\mathrm{d}w} < 0. \qquad [10]$$

[¶]One also requires that if changes in v or w dominate one process then they dominate all processes.

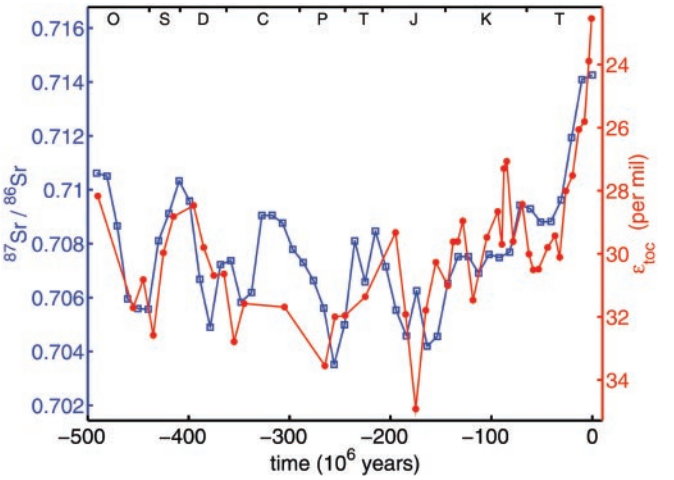

Fig. 3. The function g (blue squares) obtained by removing the memory flux from the $^{87}Sr/^{86}Sr$ data of Fig. 1, along with $\varepsilon_{\mathrm{toc}}$ (red circles). Note that the range of the $^{87}Sr/^{86}Sr$ curve is approximately five times greater than in Fig. 1. The data are plotted such that the mean of both time series lies on the same horizontal line and their rms fluctuations have the same vertical extent.

Thus the shared fluctuations of g and $\varepsilon_{\mathrm{toc}}$ indicate the relative fluctuations of ancient CO_2 levels.[‖]

Estimation of the CO_2 Signal

I proceed to estimate the CO_2 signal explicitly. First, the highest measurement of $\varepsilon_{\mathrm{toc}}$, at -175 My, is dropped because of its statistical insignificance (3). I then transform $g(t) \rightarrow \varepsilon_g(t)$, a strontium-derived estimate of $\varepsilon_{\mathrm{toc}}$, by mapping the left axis of Fig. 3 to the corresponding value on the right axis. The quantities $\varepsilon_{\mathrm{toc}}$ and ε_g are then averaged to obtain

$$\zeta(t_i) = [\varepsilon_g(t_i) + \varepsilon_{\mathrm{toc}}(t_i)]/2. \qquad [11]$$

The times t_i are given by the points where $\varepsilon_{\mathrm{toc}}$ is specified and $\varepsilon_g(t_i)$ is obtained by linear interpolation. Here it is implicitly assumed that $\varepsilon_{\mathrm{toc}}$ and ε_g contain a common signal that is enhanced by averaging. Statistical arguments suggest that ζ's rms signal-to-noise ratio lies between about 2 and 3.[**]

Assume now that Γ and ε_0 are constant and define the dimensionless CO_2 concentration $\phi = \Phi\varepsilon_0/\Gamma$ (8). In terms of ϕ and ζ, Eq. **1** then yields

$$\phi(t) = \frac{\varepsilon_0}{\varepsilon_0 - \zeta(t)}. \qquad [12]$$

At long time scales such that the oceans are in equilibrium with the atmosphere, the partial pressure pCO_2 is proportional to ϕ (1). The relative fluctuations of pCO_2 are therefore given by $\phi(t)/\phi(0)$, which is plotted in Fig. 4 for $\varepsilon_0 = 36$ per mil (‰).

[‖]Because Φ can also depend on other processes b such as organic carbon burial, the shared fluctuations of g and $\varepsilon_{\mathrm{toc}}$ do not necessarily reflect the full evolution of Φ but rather the "partial" contribution of v and w alone. However, the good correlation of Fig. 3 indicates that b's influence on Φ's fluctuations has been small, except possibly in the Carboniferous. Thus one may conclude that the fluctuations of g and $\varepsilon_{\mathrm{toc}}$ follow to good approximation the fluctuations of Φ with opposite signs.

[**]To estimate the signal-to-noise ratio of the time series $\zeta(t)$ defined by Eq. **11**, assume that $\varepsilon_{\mathrm{toc}}$ and ε_g are each composed of a shared but unknown signal z in the presence of zero-mean noise η_{toc} and η_g, respectively: $\varepsilon_{\mathrm{toc}} = z + \eta_{\mathrm{toc}}$ and $\varepsilon_g = z + \eta_g$. The quantity ζ is an estimate of z. Its signal-to-noise ratio may be computed under the assumption that η_{toc} and η_g each have variance σ_η^2, z has variance σ_z^2, and η_{toc}, η_g, and z are each uncorrelated to the other. The expectation of the correlation coefficient R is then $\sigma_z^2/(\sigma_z^2 + \sigma_\eta^2)$ (25). The observed correlation $|R| = 0.80$ then yields $\sigma_z^2/\sigma_\eta^2 = 4$, or that the rms signal fluctuation is twice that of the noise. The rms signal-to-noise ratio of ζ can be as large as a factor of $\sqrt{2}$ greater, i.e., it should range between about 2 and 3.

GEOLOGY

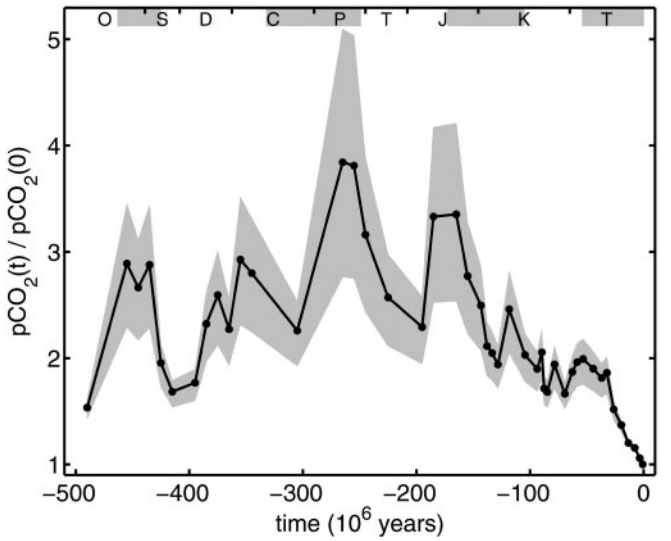

Fig. 4. Fluctuations of pCO_2 for the last 500 My, normalized by the estimate of pCO_2 obtained from the most recent value of ζ. The solid line is obtained from Eq. **12** by using $\varepsilon_0 = 36‰$. The lower and upper limits of the gray area surrounding the pCO_2 curve result from $\varepsilon_0 = 38$ and 35‰, respectively. The gray bars at the top correspond to periods when Earth's climate was relatively cool; the white spaces between them correspond to warm modes (18).

The gray area surrounding the pCO_2 curve in Fig. 4 brackets this result for $\varepsilon_0 = 35‰$ and 38‰, a range consistent with previous estimates (3).

Fig. 4 reveals that CO_2 levels have mostly decreased for the last 175 My. Prior to that point they appear to have fluctuated from about two to four times modern levels with a dominant period of about 100 My. The decline for the last 175 My is also present in several previous pCO_2 reconstructions (7, 8, 26, 27), and the entire curve displays some similarity to a previous estimate derived from the geologic record of carbonate formation (26). Although the period before −175 My differs substantially from previous geochemical model calculations (7), an approximate error estimate lends considerable credence to the pCO_2 curve of Fig. 4. Specifically, ϕ should inherit ζ's signal-to-noise ratio of 2–3. This correspondence would be exact if $\phi(\zeta)$ were linear. Because $\phi(\zeta)$ is monotonic for the observed range of ζ, its nonlinearity does not affect the timing of the maxima and minima of the pCO_2 curve. Thus the linear error estimate remains pertinent.

Comparison with the Climate Record

Using a variety of sedimentological criteria, Frakes *et al.* (18) have concluded that Earth's climate has cycled several times between warm and cool modes for roughly the last 600 My. Recent work by Veizer *et al.* (28), based on measurements of oxygen isotopes in calcite and aragonite shells, appears to confirm the existence of these long-period (~135 My) climatic fluctuations. Changes in CO_2 levels are usually assumed to be among the dominant mechanisms driving such long-term climate change (29).

It is therefore interesting to ask what, if any, correspondence exists between ancient climate and the estimate of pCO_2 in Fig. 4. The gray bars at the top of Fig. 4 correspond to the periods when the global climate was cool; the intervening white space corresponds to the warm modes (18). The most recent cool period corresponds to relatively low CO_2 levels, as is widely expected (30). However, no correspondence between pCO_2 and climate is evident in the remainder of the record, in part because the apparent 100 My cycle of the pCO_2 record does not match the longer climatic cycle. The lack of correlation remains if one calculates the change in average global surface temperature resulting from changes in pCO_2 and the solar constant using energy-balance arguments (7, 26).

Superficially, this observation would seem to imply that pCO_2 does not exert dominant control on Earth's climate at time scales greater than about 10 My. A wealth of evidence, however, suggests that pCO_2 exerts at least *some* control [see Crowley and Berner (30) for a recent review]. Fig. 4 cannot by itself refute this assumption. Instead, it simply shows that the "null hypothesis" that pCO_2 and climate are unrelated cannot be rejected on the basis of this evidence alone.

Discussion and Conclusion

One of the principal contributions of this study is methodological. From observations of a weak correlation between strontium and carbon isotopic signals (Fig. 1) and their shared dependence on global weathering rates and magmatic activity, weathering and magmatism are deduced to be the main processes driving the signals' fluctuations. Correction for the effects of sedimentary recycling enhances the correlation (Fig. 3), indicates a strong shared signal, and strengthens this conclusion.

A second, crucial step is to note that any quantity with a similar joint dependence on weathering and magmatic processes may be expected to display similar fluctuations. Here attention has been focused on CO_2 levels; as for the strontium and carbon isotopic signals, CO_2 levels depend on weathering and magmatism with opposite signs and should therefore fluctuate roughly in sync with the isotopic signals. Because the reasoning is general, it need not be limited to CO_2. Among the many possible applications, the case of oceanic phosphate concentrations is particularly interesting. Phosphate concentrations should increase with weathering and decrease with hydrothermal activity (31); thus the methodology in this paper may be applicable to their reconstruction. Moreover, because phosphorus is a limiting nutrient, oceanic productivity may be expected to covary positively with its concentration in seawater, suggesting that CO_2 levels and productivity covary negatively at geologic time scales (8).

Such reasoning naturally raises the issue of cause and effect. This study indicates that degassing and silicate weathering were the primary controls on the carbon cycle for the last 500 My. But the results do not themselves indicate whether either of these mechanisms dominated, or whether weathering was driven by the diversification of land plants (8), continental collisions (9), or a complex combination of tectonic, biological, and geochemical processes (7). They do, however, offer a new view of the long-term fluctuations of pCO_2 that will hopefully stimulate novel approaches to the study of biogeochemical cycles at evolutionary time scales.

I thank O. Aharonson, L. Derry, J. Hayes, P. Hoffman, A. Knoll, L. Kump, J. Sachs, R. Summons, and the late John Edmond for helpful remarks. This work was supported in part by National Science Foundation Grant DEB-0083983.

1. Walker, J. C. G. (1977) *Evolution of the Atmosphere* (Macmillan, New York).
2. Holland, H. D. (1978) *The Chemistry of the Atmosphere and Oceans* (Wiley, New York).
3. Hayes, J. M., Strauss, H. & Kaufman, A. J. (1999) *Chem. Geol.* **161,** 103–125.
4. Veizer, J., Ala, D., Azmy, D., Bruckschen, P., Buhl, D., Bruhn, F., Carden, G., Diener, A., Ebneth, S., Godderis, Y., *et al.* (1999) *Chem. Geol.* **161,** 59–88.
5. Freeman, K. & Hayes, J. M. (1992) *Global Biogeochem. Cycles* **6,** 185–198.
6. Francois, L. M. & Walker, J. C. G. (1992) *Am. J. Sci.* **292,** 81–135.
7. Berner, R. A. (1994) *Am. J. Sci.* **294,** 56–91.
8. Rothman, D. H. (2001) *Proc. Natl. Acad. Sci. USA* **98,** 4305–4310.
9. Edmond, J. (1992) *Science* **258,** 1594–1597.
10. Richter, F. M., Rowley, D. B. & DePaolo, D. J. (1992) *Earth Planet. Sci. Lett.* **109,** 11–23.
11. Hayes, J. M. (1993) *Marine Geol.* **113,** 111–125.

12. Derry, L. A. & France-Lanord, C. (1996) *Earth Planet. Sci. Lett.* **142,** 59–74.
13. Quade, J., Roe, L., DeCelles, P. G. & Ojha, T. P. (1997) *Science* **276,** 1828–1831.
14. Sharma, M., Wasserburg, G. J., Hofmann, A. & Chakrapani, G. J. (1999) *Geochim. Cosmochim. Acta* **63,** 4005–4012.
15. Basu, A. R., Jacobsen, S. B., Poreda, R. J., Dowling, C. B. & Aggarwal, P. K. (2001) *Science* **293,** 1470–1473.
16. Garrels, R. M. & Mackenzie, F. T. (1971) *Evolution of Sedimentary Rocks* (Norton, New York).
17. Brass, G. W. (1976) *Geochim. Cosmochim. Acta* **40,** 721–730.
18. Frakes, L. A., Francis, J. E. & Syktus, J. I. (1992) *Climate Modes of the Phanerozoic* (Cambridge Univ. Press, Cambridge, U.K.).
19. Walter, M. R., Veevers, J. J., Calver, C. R., Gorjan, P. & Hill, A. C. (2000) *Precambrian Res.* **100,** 371–433.
20. Vio, R., Strohmer, T. & Wamsteker, W. (2000) *Publ. Astrono. Soc. Pac.* **112,** 74–90.
21. Press, W. H., Flannery, B. P., Teukolsky, S. A. & Vetterling, W. T. (1995) *Numerical Recipes in C: The Art of Scientific Computing* (Cambridge Univ. Press, Cambridge, U.K.).
22. Popp, B. N., Laws, E. A., Bidigare, R. R., Dore, J. E., Hanson, K. L. & Wakeham, S. G. (1998) *Geochim. Cosmochim. Acta* **62,** 69–77.
23. Palmer, M. R. & Edmond, J. (1989) *Earth Planet. Sci. Lett.* **92,** 11–26.
24. Urey, H. C. (1952) *The Planets* (Yale Univ. Press, New Haven, CT).
25. Feller, W. (1968) *An Introduction to Probability Theory and Its Applications* (Wiley, New York).
26. Budyko, M. I., Ronov, A. B. & Yanshin, A. L. (1987) *History of the Earth's Atmosphere* (Springer, Berlin).
27. Ekart, D. D., Cerling, T. E., Montanez, I. P. & Tabor, N. J. (1999) *Am. J. Sci.* **299,** 805–827.
28. Veizer, J., Godderis, Y. & Francois, L. M. (2000) *Nature (London)* **408,** 698–701.
29. Kump, L. R. (2000) *Nature (London)* **408,** 651–652.
30. Crowley, T. J. & Berner, R. A. (2001) *Science* **292,** 870–872.
31. Wheat, C. G., Feely, R. A. & Mottl, M. J. (1996) *Geochim. Cosmochim. Acta* **60,** 3593–3608.
32. Harland, W. B., Armstrong, R., Cox, A., Craig, L., Smith, A. G. & Smith, D. G. (1990) *A Geologic Time Scale 1989* (Cambridge Univ. Press, Cambridge, U.K.).